Acta Crystallographica Section F
Structural Biology and Crystallization Communications
ISSN 1744-3091

Crystallization and preliminary X-ray analysis of the stress-response PPM phosphatase RsbX from *Bacillus subtilis*

Masatoshi Suganuma,[a] Aik Hong Teh,[b] Masatomo Makino,[b] Nobutaka Shimizu,[b] Tomonori Kaneko,[a]‡ Kunio Hirata,[c] Masaki Yamamoto[c] and Takashi Kumasaka[b,c]*

[a]Department of Life Science, Tokyo Institute of Technology, Japan, [b]Japan Synchrotron Radiation Research Institute (SPring-8/JASRI), Japan, and [c]RIKEN SPring-8 Center, Japan

‡ Present address: Schulich School of Medicine and Dentistry, University of Western Ontario, Canada.

Correspondence e-mail: kumasaka@spring8.or.jp

Received 1 June 2009
Accepted 25 September 2009

RsbX from *Bacillus subtilis* is a manganese-dependent PPM phosphatase and negatively regulates the signal transduction of the general stress response by the dephosphorylation of RsbS and RsbR, which are activators of the alternative RNA polymerase σ factor SigB. In order to elucidate the structural–functional relationship of its Ser/Thr protein-phosphorylation mechanism, an X-ray crystallographic diffraction study of RsbX was performed. Recombinant RsbX was expressed in *Escherichia coli*, purified and crystallized. Crystals were obtained using the sitting-drop vapour-diffusion method and X-ray diffraction data were collected to 1.06 Å resolution with an $R_{\rm merge}$ of 8.1%. The crystals belonged to the triclinic space group $P1$, with unit-cell parameters a = 33.3, b = 41.7, c = 68.6 Å, α = 98.8, β = 90.0, γ = 108.4°.

1. Introduction

Once optimal bacterial growth conditions have been interrupted by nutrient depletion or deterioration of the environment such as an accumulation of metabolic pollutants, bacteria enter the stationary phase, in which cell growth and division slow and their cellular metabolism and cell contents change to resist growth-limiting stresses.

In the representative Gram-positive bacterium *Bacillus subtilis*, it is known that an alternative σ factor, SigB ($\sigma^{\rm B}$), is the regulator of the general stress response (Haldenwang, 1995; Hecker & Volker, 1998; Price *et al.*, 2001; Guedon *et al.*, 2003). The activity of SigB is directly regulated by a signalling cascade under stress conditions derived from both nutrient deprivation and environmental changes and the cascade is composed of seven components called Rsb proteins (regulators of sigma B; Hecker *et al.*, 2007). These components transduce the stress signal to SigB by a series of phosphorylation–dephosphorylation and accompanying protein association–dissociation events. The environmental stress triggers activation of the supramolecular protein-complex stressosome, which contains multiple copies of the RsbR, RsbS and RsbT proteins (Chen *et al.*, 2003; Marles-Wright *et al.*, 2008). The downstream cascade of the activated stressosome releases SigB from the anti-sigma factor RsbW and induces the stress response. Here, we focus on RsbX, which deactivates the stressosome by the dephosphorylation of RsbS and/or RsbR (Boylan *et al.*, 1992).

RsbX is composed of 199 amino acids and its sequence indicates that it is comprised of only an Mg^{2+}- or Mn^{2+}-dependent protein phosphatase (PPM) catalytic domain. PPM is known to be a dinuclear metalloenzyme similar to phosphoprotein phosphatase (PPP) and works in a wide variety of intracellular phosphorylation/dephosphorylation signalling cascades by responding to stimuli (Taylor & Zhulin, 1999). This family is divided into subfamilies I and II based on amino-acid sequences (Bork *et al.*, 1996; Shi, 2004). Subfamily I enzymes are composed of 11 conserved sequence motifs and are widely distributed in eukaryotes (*e.g.* human PP2C) and prokaryotes. Recent structural analyses revealed the presence of an additional third metal ion in their active centres (Pullen *et al.*, 2004; Bellinzoni *et al.*, 2007; Rantanen *et al.*, 2007; Wehenkel *et al.*, 2007; Schlicker *et al.*, 2008). Binding of the third metal contributes to repositioning of the

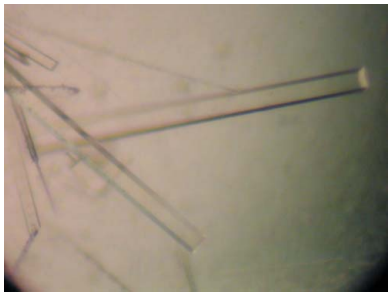

flap subdomain containing the amino-acid ligands of the third metal and is considered to control substrate binding as the subdomain is located beside the active site. In contrast, structures of subfamily II, which includes RsbX and the other *Bacillus* phosphatases RsbU, RsbP and SpoIIE, have not yet been determined. Interestingly, their sequences lack the 5a/5b motif which forms the flap subdomain in PPM subfamily I (Shi, 2004). The lack of this motif suggests potential differences between the two subfamilies in terms of binding of the third metal and substrate recognition. With regard to metal binding, a DNA microarray study of RsbU mutants indicated that metal binding regulates phosphatase activity (Guedon *et al.*, 2003), revealing that an increasing manganese concentration induces general stress response in the wild type, but no response was detected in the mutants.

Owing to the lack of structural information for this subfamily, it would be of special interest to investigate the actual metal-binding mode by structural determination of RsbX. Moreover, the recently solved structure of an RsbS orthologue (Marles-Wright *et al.*, 2008) should provide insight into the enzyme–substrate interaction between RsbX and RsbS. The RsbS orthologue structure was typical of the sulfate transporter and anti-sigma (STAS) family and showed that its phospholylated Ser is located in a loop region protruding into solvent, which might be suitable for direct interaction with RsbX.

To elucidate the structural basis of substrate recognition and the dephosphorylation mechanism of PPM subfamily II phosphatases and to reveal the structural and functional relationship between the three paralogues (RsbX, RsbP and RsbU), structural analysis of RsbX is under way. In the present paper, we describe the molecular cloning, expression, purification, crystallization and preliminary X-ray diffraction analysis of RsbX.

2. Cloning, expression and purification

The gene coding *rsbX* was cloned from a single colony of *B. subtilis* strain 168 by the colony PCR method using the primers 5′-GGTGG-TT**GCTCTTC**CAACATGATCCAGGTTGAAGAAA-3′ and 5′-G-GTGGT**CTCGAG**TTAGGACAGCTGTCCGAGAAT-3′ (*Sap*I and *Xho*I recognition sites, respectively, are shown in bold). The PCR product was inserted into the *Escherichia coli* expression vector pTYB11 (New England Biolabs) between the *Sap*I and *Xho*I sites and the sequence of the resulting plasmid, pTYB11-RsbX, was verified. To express RsbX, *E. coli* BL21 (DE3) (Novagen) was transformed with pTYB11-RsbX and cultured in Luria–Bertani medium containing 50 µg ml^{-1} ampicillin at 310 K until the optical density (OD_{600}) of the culture reached ∼0.7. The cells were then induced with 1.0 m*M* isopropyl *β*-D-1-thiogalactopyranoside and allowed to grow overnight at 291 K.

All the following purification procedures were conducted at 277 K. The cultures were centrifuged at 4000*g* for 15 min. The harvested cell pellets were suspended in phosphate-buffered saline (Sigma–Aldrich), re-collected by centrifugation at 4000*g* for 15 min and stored at 193 K.

The stored cells were resuspended in buffer *A* (50 m*M* Tris–HCl pH 8.0, 0.5 *M* NaCl, 1 m*M* DTT) and disrupted by sonication. The suspension was centrifuged at 20 000*g* for 1 h to remove cell debris. The supernatant was loaded onto chitin beads (30 ml; New England Biolabs) that had been equilibrated in buffer *A*. After washing the resin with five column volumes of buffer *A*, an intein-mediated cleavage reaction of the fusion protein was induced by the addition of buffer *A* containing 70 m*M* DTT for 2 d. The eluted fractions were concentrated using an Amicon Ultra-15 Centrifugal Filter Unit with an Ultracel-10 membrane (Millipore) and further purified by size-exclusion chromatography on a HiLoad Superdex 75 16/80 column (GE Healthcare) in buffer *B* (50 m*M* Tris–HCl pH 8.0, 0.2 *M* NaCl, 1 m*M* DTT) using an ÄKTA FPLC system (GE Healthcare). The purified protein solution was pooled and concentrated to a protein concentration of 10 mg ml^{-1} using a Microcon YM-10 membrane filter (Millipore). The protein concentration was estimated using a spectrophotometer with a specific absorption coefficient ε_{280} of 13 410 M^{-1} cm^{-1} calculated using the *ProtParam* server (Gasteiger *et al.*, 2005).

Table 1
Data-processing statistics for RsbX.

Values in parentheses are for the outermost resolution shell.

Space group	*P*1
Wavelength (Å)	1.0000
Unit-cell parameters (Å, °)	a = 33.3, b = 41.7, c = 68.6, α = 98.8, β = 90.0, γ = 108.4
Protein molecules in ASU	2
V_M (Å^3 Da^{-1})	2.0
Solvent content (%)	39.0
Resolution range (Å)	67.73–1.06 (1.10–1.06)
Total observations	515582
Unique reflections	141658
Redundancy	3.6 (2.5)
Completeness (%)	90.3 (71.5)
Mean $I/\sigma(I)$	23.6 (2.3)
R_{merge}† (%)	8.1 (36.6)

† $R_{merge} = \sum_{hkl}\sum_i |I_i(hkl) - \langle I(hkl)\rangle| / \sum_{hkl}\sum_i I_i(hkl)$, where $I_i(hkl)$ is the ith observation of reflection hkl and $\langle I(hkl)\rangle$ is the weighted average intensity for all observations of reflection hkl.

3. Crystallization and preliminary X-ray analysis

Initial crystallization conditions were screened by the sitting-drop vapour-diffusion method at 293 K using the commercially available sparse-matrix screening kits Wizard Screens I and II (Emerald Bio-Structures). Drops were formed by mixing 1 µl 10 mg ml^{-1} protein solution and 1 µl reservoir solution and were equilibrated against 100 µl reservoir solution. Crystals were grown from various conditions containing polyethylene glycols and divalent metal ions. In particular, large crystals were grown in a few days from a solution consisting of 0.1 *M* Tris–HCl pH 8.5, 5 m*M* $MnCl_2$, 25%(*w*/*v*) PEG 1000 using the microseeding technique with seed crystals obtained from 0.1 *M* Tris–HCl pH 8.5, 5 m*M* $MgCl_2$, 20%(*w*/*v*) PEG 1000.

X-ray data collection was carried out on the SPring-8 BL41XU beamline using a Rayonix MX225HE CCD detector. The crystals were flash-cooled in a cold nitrogen-gas stream without first being

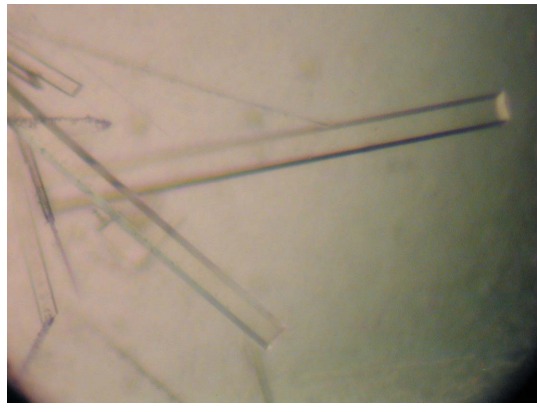

Figure 1
Crystals of RsbX. The maximum dimensions of the crystals were approximately 0.70 × 0.05 × 0.02 mm.

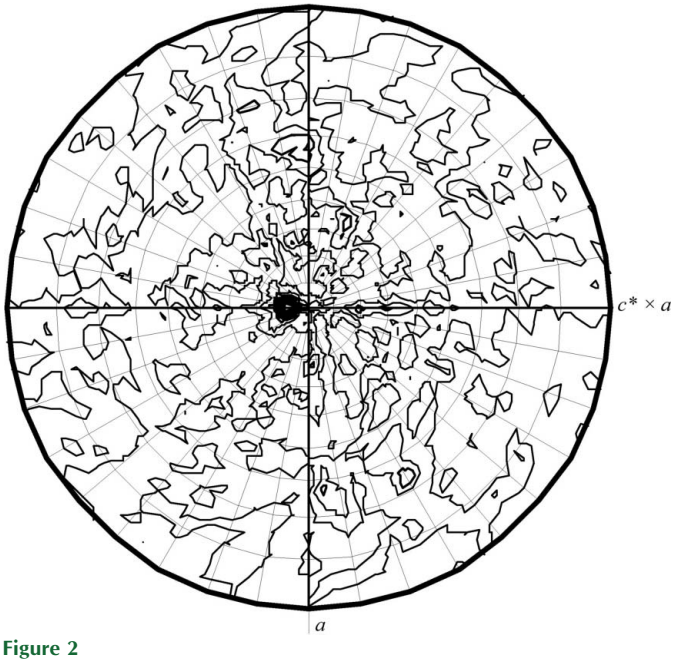

Figure 2
Self-rotation function at the $\chi = 180^\circ$ section. The map was calculated in the resolution range 50–4 Å with an integration radius of 25 Å and drawn with contour intervals of 0.5σ. A significant peak was observed at the position $\theta = 170.9^\circ$, $\omega = 90.0^\circ$, $\chi = 180.0^\circ$. The figure was drawn with *CCP*4/*MOLREP* (Collaborative Computational Project, Number 4, 1994).

transferred to cryoprotectant solution. A wavelength of 1.0 Å, a beam size of 10 µm diameter and a crystal-to-detector distance of 75 mm were used. A total of 360 images were collected with an oscillation angle of 1° and an exposure time of 2.0 s per image. The beam irradiation position was scanned gradually along the longest axis of the bar-shaped crystals using the SPring-8 data-collection software *BSS* (Ueno *et al.*, 2005; Hasegawa *et al.*, personal communication). The 10 µm diameter beam and the change in irradiation position led to mitigation of radiation damage. The data were integrated and scaled using the *HKL*-2000 program package (Otwinowski & Minor, 1997). Data-processing statistics are listed in Table 1.

4. Results and discussion

The RsbX protein was overexpressed in *E. coli* cells using the pTYB11 vector and contained no artificial amino acids after digestion of the intein tag. The enzyme was highly purified by two steps of chromatography with a yield of 1.2 mg per litre of culture. The enzyme activity of the purified sample was detected using *p*-nitrophenyl phosphate as a substrate, showing that the enzyme required Mn^{2+} ions for the catalytic reaction (data not shown).

RsbX was crystallized under the conditions described above and crystals grew to maximal dimensions of 0.70 × 0.05 × 0.02 mm (Fig. 1). A crystal diffracted to 1.06 Å resolution and belonged to the triclinic space group *P*1, with unit-cell parameters $a = 33.3$, $b = 41.7$, $c = 68.6$ Å, $\alpha = 98.8$, $\beta = 90.0$, $\gamma = 108.4^\circ$. Assuming that the unit cell contained two monomers, the Matthews coefficient was estimated as 2.0 $Å^3\ Da^{-1}$ and the solvent content was 39%. This estimation is supported by the Matthews coefficient probability (Kantardjieff & Rupp, 2003) and the self-rotation function, which shows the existence of a twofold axis almost along the *c* axis (Fig. 2). The dimer formed in the unit cell might not be related to the physiological state, as the elution profile of the size-exclusion chromatography showed a monomeric state of the protein in solution (data not shown).

Molecular-replacement trials using several structural models of PPM/PP2C phosphatases failed as the existing models did not belong to PPM subfamily II and had relatively low sequence similarity (∼15%) to RsbX. Thus, structure determination using anomalous dispersion of native manganese or other substituted metal ions and structural model refinement are under way.

This research was supported in part by a Grant-in-Aid for Scientific Research (C) (19570102) from the Ministry of Education, Culture, Sports, Science and Technology (MEXT), Japan. The synchrotron-radiation experiments were performed on beamline BL41XU at SPring-8 with the approval of the Japan Synchrotron Radiation Research Institute (JASRI; Proposal No. 2008A1233).

References

Bellinzoni, M., Wehenkel, A., Shepard, W. & Alzari, P. M. (2007). *Structure*, **15**, 863–872.
Bork, P., Brown, N. P., Hegyi, H. & Schultz, J. (1996). *Protein Sci.* **5**, 1421–1425.
Boylan, S. A., Rutherford, A., Thomas, S. M. & Price, C. W. (1992). *J. Bacteriol.* **174**, 3695–3706.
Chen, C. C., Lewis, R. J., Harris, R., Yudkin, M. D. & Delumeau, O. (2003). *Mol. Microbiol.* **49**, 1657–1669.
Collaborative Computational Project, Number 4 (1994). *Acta Cryst.* D**50**, 760–763.
Gasteiger, E., Hoogland, C., Gattiker, A., Duvaud, S., Wilkins, M. R., Appel, R. D. & Bairoch, A. (2005). *The Proteomics Protocols Handbook*, edited by J. M. Walker, pp. 571–607. Totowa: Humana Press.
Guedon, E., Moore, C. M., Que, Q., Wang, T., Ye, R. W. & Helmann, J. D. (2003). *Mol. Microbiol.* **49**, 1477–1491.
Haldenwang, W. G. (1995). *Microbiol. Rev.* **59**, 1–30.
Hecker, M., Pane-Farre, J. & Volker, U. (2007). *Annu. Rev. Microbiol.* **61**, 215–236.
Hecker, M. & Volker, U. (1998). *Mol. Microbiol.* **29**, 1129–1136.
Kantardjieff, K. A. & Rupp, B. (2003). *Protein Sci.* **12**, 1865–1871.
Marles-Wright, J., Grant, T., Delumeau, O., van Duinen, G., Firbank, S. J., Lewis, P. J., Murray, J. W., Newman, J. A., Quin, M. B., Race, P. R., Rohou, A., Tichelaar, W., van Heel, M. & Lewis, R. J. (2008). *Science*, **322**, 92–96.
Otwinowski, Z. & Minor, W. (1997). *Methods Enzymol.* **276**, 307–326.
Price, C. W., Fawcett, P., Ceremonie, H., Su, N., Murphy, C. K. & Youngman, P. (2001). *Mol. Microbiol.* **41**, 757–774.
Pullen, K. E., Ng, H. L., Sung, P. Y., Good, M. C., Smith, S. M. & Alber, T. (2004). *Structure*, **12**, 1947–1954.
Rantanen, M. K., Lehtio, L., Rajagopal, L., Rubens, C. E. & Goldman, A. (2007). *FEBS J.* **274**, 3128–3137.
Schlicker, C., Fokina, O., Kloft, N., Grune, T., Becker, S., Sheldrick, G. M. & Forchhammer, K. (2008). *J. Mol. Biol.* **376**, 570–581.
Shi, L. (2004). *Front. Biosci.* **9**, 1382–1397.
Taylor, B. L. & Zhulin, I. B. (1999). *Microbiol. Mol. Biol. Rev.* **63**, 479–506.
Ueno, G., Kanda, H., Kumasaka, T. & Yamamoto, M. (2005). *J. Synchrotron Rad.* **12**, 380–384.
Wehenkel, A., Bellinzoni, M., Schaeffer, F., Villarino, A. & Alzari, P. M. (2007). *J. Mol. Biol.* **374**, 890–898.